JOURNAL OF MATERIALS SCIENCE 25 (1990) 1765–1772

Investigation of electrical and photoluminescent properties of MBE-grown $Al_xGa_{1-x}As$ layers

W. C. LIU
Department of Electrical Engineering, National Cheng Kung University, Tainan, Taiwan

The electrical and photoluminescent (PL) properties of $Al_xGa_{1-x}As$ layers grown by MBE have been investigated. Some experimental factors, e.g. vacuum conditions, substrate growth temperature and As/group-III flux ratio, have been considered. Undoped AlGaAs layers exhibit slight p-type characteristics due to C accepters and its concentration is lower than $10^{15}\,cm^{-3}$. Both n- and p-type AlGaAs layers achieve semi-insulated high resistance when the substrate temperature is lower than 580° C. The experimental results are comparable to other reports. In summary, the excellent vacuum environment, higher substrate temperature (T_s > 580° C) and lower As/group-III flux ratio are the necessary conditions for growing high quality $Al_xGa_{1-x}As$ layers.

1. Introduction

Recently, due to the continuous development and fabrication on MBE-grown GaAs–$Al_xGa_{1-x}As$ heterostructure devices (e.g. lasers, high-speed transistors), AlGaAs has become a very important material for device applications [1–6].

From the point of view of technique, the growth of $Al_xGa_{1-x}As$ layers is more difficult than GaAs layers. The $Al_xGa_{1-x}As$ layer is so active that it reacts easily with environmental elements. During the growth process, if the ultra-high vacuum conditions of MBE system are not good, oxygen and carbon contamination are present in the form of residual gases (CO, H_2O, O_2). This will introduce a serious degradation of the quality of the $Al_xGa_{1-x}As$ layers. Possibly, the $Al_xGa_{1-x}As$ layers may achieve semi-insulated high resistance. On the other hand, the growth temperature and As/group-III flux ratio also play important roles in $Al_xGa_{1-x}As$ layer properties [7, 8]. In this paper, the influence of these factors on the MBE-grown $Al_xGa_{1-x}As$ layers using the electrical and photoluminescent measurements is reported.

2. Electrical characteristics of $Al_xGa_{1-x}As$ layers

2.1. n-type $Al_xGa_{1-x}As$

In the MBE growth, silicon is widely used as n-type dopant because a very sharp impurity distribution profile can be obtained [9]. Normally, the sticking coefficient of silicon is unity, so the doping concentration is dependent on the quantities of silicon atoms arriving at the substrate. Therefore, the doping concentration is proportional to the silicon vapour pressure [10]. Figure 1 shows the dependence of silicon cell temperature on the free electron concentration of silicon-doped $Al_{0.26}Ga_{0.74}As$ layers. The growth temperature was kept at 620° C, and the GaAs growth rate was $1.1\,\mu m\,h^{-1}$. Basically, the variation in AlGaAs is similar to the trend for the silicon vapour pressure. In addition, the carrier concentration of AlGaAs is less than GaAs under the same growth conditions, due to the less effective group-III vacancies existing in the AlGaAs layers. So the opportunities for occupation of silicon is reduced and the free electron concentration is reduced simultaneously. The highest concentration was $3 \times 10^{18}\,cm^{-3}$. When the silicon cell temperature was raised further, the electron concentration is reduced due to the auto-compensation effect [11]. Experimental data were obtained from Hall effect and Van der Paul measurements.

Because silicon is a group IV element, it is an amphoteric dopant for III–V compounds. The amphoteric-doping phenomenon can be explained by the following equations

$$Si_{(g)} + V_{As} \rightleftharpoons Si_{As} \rightleftharpoons Si_{As^-} + h^+$$

$$Si_{(g)} + V_{III} \rightleftharpoons Si \rightleftharpoons Si_{III+} + e^-$$

$$V_{III} + Si_{III} \rightleftharpoons V_{III}Si_{III} \rightleftharpoons V_{III}Si_{III^-} + h^+ \quad (1)$$

where $V_{III}Si_{III}$ is a silicon complex. In most MBE growth, the arsenic-rich condition is adopted. More group-III (Al, Ga) vacancies exist, i.e. the opportunity for silicon atoms to occupy the group-III vacancies is larger than that for arsenic vacancies. So, silicon exhibits donor characteristics. On the other hand, if more arsenic vacancies occur, silicon provides p-type acceptor characteristics. Therefore, the growth conditions (e.g. growth temperature and As/(Ga + Al) flux ratio, etc.) will affect the doping characteristics.

Figure 2 shows the dependence of free electron concentration on electron mobility of silicon-doped AlGaAs layers at room temperature. The aluminium mole fraction was fixed at $x = 0.26$ and 0.35, respectively. Due to alloy scattering, the mobility is less than GaAs, on average. The mobility decreases with increasing aluminium mole fraction, x. Basically, our experimental data are comparable with other liquid phase epitary (LPE) or vapour phase epitary (VPE) grown

0022–2461/90 $03.00 + .12

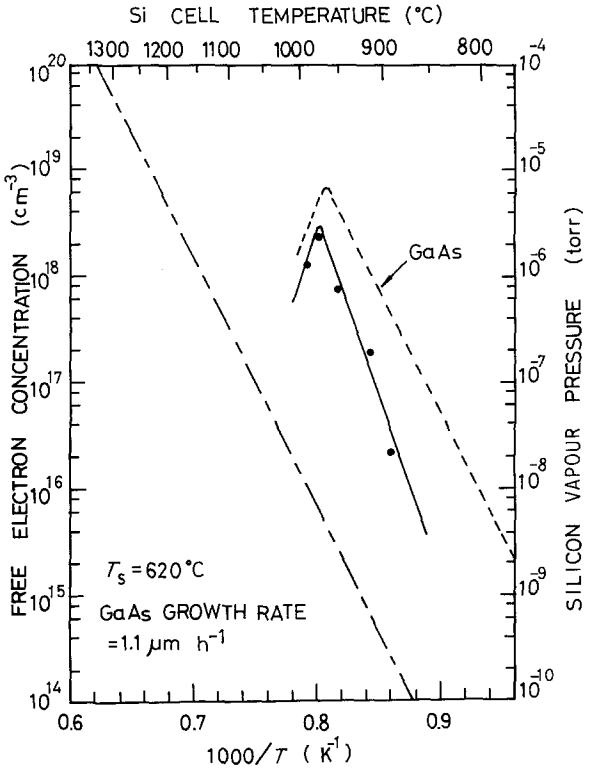

Figure 1 Characteristics of silicon-doped $Al_{0.20}Ga_{0.74}As$ layers at 300 K (---) silicon vapour pressure, (– – –) characteristics of silicon-doped GaAs layers.

AlGaAs layers [12, 13]. The relationship between carrier density and mobility at 77 K is drawn in Fig. 3. At low temperature, the electron mobility is increased significantly due to the reduction of phonon scattering. In addition, the carrier concentration is decreased relatively as a result of the freeze-out effect.

Figure 4 demonstrates the influence of substrate temperature on the doping concentration and carrier mobility of $Al_{0.26}Ga_{0.74}As$ layers. The silicon cell temperature was fixed at 910° C, and the arsenic partial pressure was kept at 1.8×10^{-7} torr. Although Chai *et al.* [14] have pointed out the arsenic sticking coefficient is decreased at high temperature, it gives rise to an increase in the number of arsenic vacancies, and the opportunity for silicon to occupy arsenic vacancies is increased, and thus the impurity concentration is, predictively, decreased. However, in our experiments, it is not valid. The doping concentration is increased with increasing substrate temperature when T_s is lower than 650° C. But when T_s is higher than 650° C, the doping concentration will decrease with increasing substrate temperature, based on [15–17]

$$V_{III} \propto e^{-E_a/KT} \tag{2a}$$

and

$$V_{As} \propto e^{-E_a KT} \tag{2b}$$

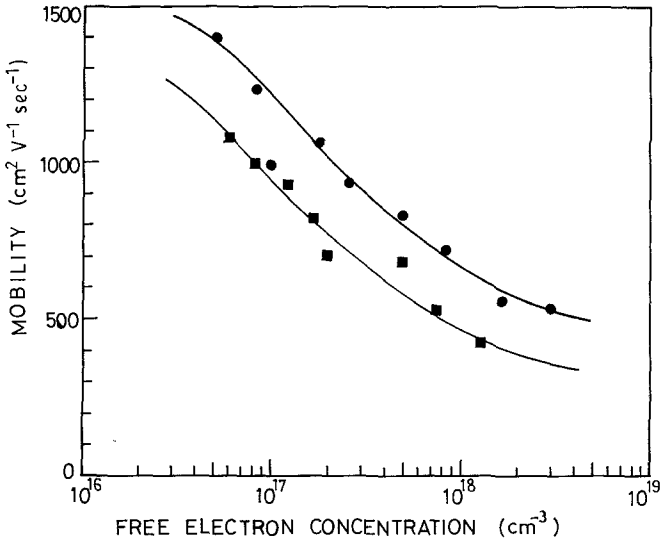

Figure 2 The relationship between the mobility and carrier concentration of silicon-doped $Al_xGa_{1-x}As$ layers at room temperature (300 K), where x = (●) 0.26, (■) 0.35.

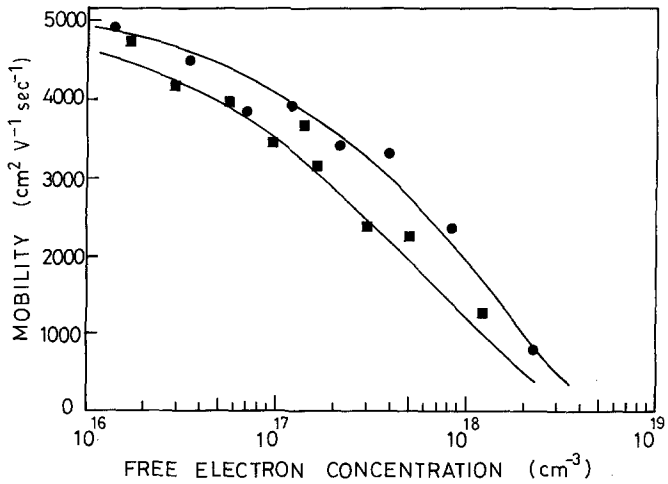

Figure 3 The relationship between the mobility and carrier concentration of silicon-doped $Al_xGa_{1-x}As$ layers at 77 K, where x = (●) 0.26, (■) 0.35.

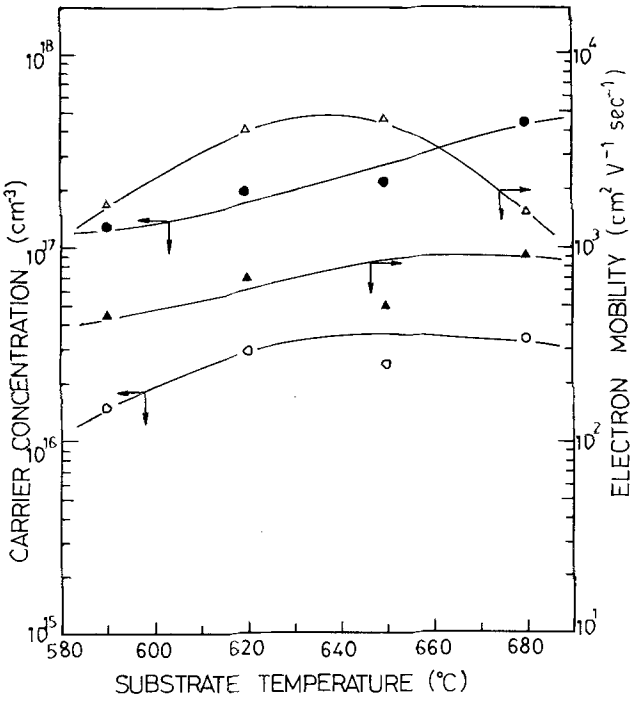

Figure 4 The influence of substrate temperature on electrical properties of silicon-doped layers: (●, ▲) 300 K, (○, △) 77 K. Silicon cell temperature = 910° C.

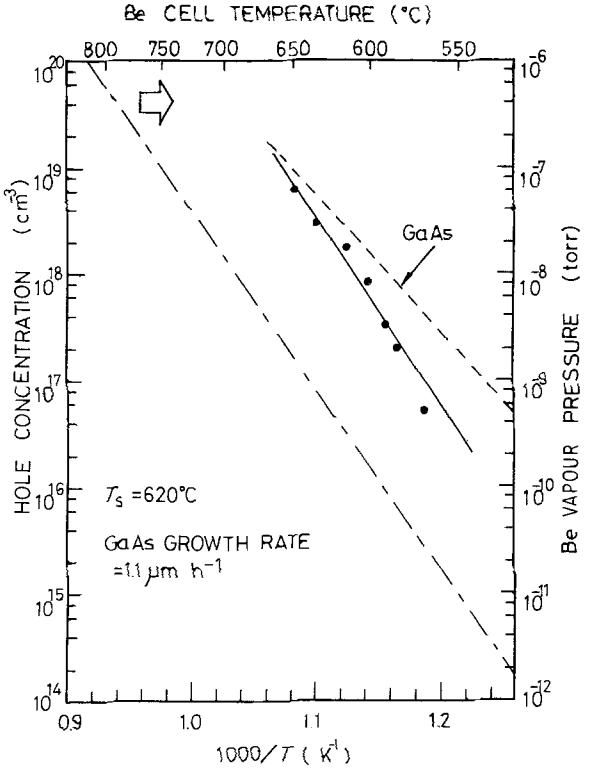

Figure 5 Hole concentration as a function of beryllium cell temperature at 300 K in beryllium-doped $Al_{0.26}Ga_{0.74}As$. (– – –) beryllium vapour pressure, (– – –) GaAs layer characteristics.

where V_{III} and V_{As} are the vacancies of group III and arsenic, respectively. At high temperature, not only the arsenic sticking coefficient but also the group III sticking coefficient will be decreased, simultaneously. As a result, the total number of vacancies is increased. Therefore, the variation in doping concentration is determined by the occupation by silicon atoms of arsenic vacancies or group III vacancies. For comparison, the experimental data are listed in Table I. It is worthwhile to note that AlGaAs layers achieve semi-insulated high resistance when the growth temperature is lower than 580° C. This is due to the existence of many deep-level traps at lower substrate temperatures. The best growth temperature ranges from 620 to 660° C. The electron mobility, μ, at 77 K can be up to 5000 cm^2 V^{-1} sec^{-1}, which is comparable with the best results obtained from other MBE systems [18, 19].

2.2. p-type $Al_xGa_{1-x}As$

Beryllium is the most common acceptor dopant used in MBE growth due to its very sharp doping profile and excellent results both for electrical and optical properties [20]. Figure 5 shows the influence of beryllium cell temperature on hole concentration. It is known that the beryllium doping concentration of $Al_{0.26}Ga_{0.74}As$ is less than that of GaAs layers under the same conditions, for the same reasons as for silicon-doped layers. Basically, the variation of beryllium doping concentration is similar to that of beryllium vapour pressure. The lowest doping concentration is about 5×10^{16} cm^{-3}. Due to the B–O effect, i.e. beryllium can easily react with CO and H_2O, the doping concentration is difficult to reduce to a greater degree. The highest doping density is up to about 1×10^{19} cm^{-3}.

Figure 6 shows the relationship between the hole concentration and mobility at 300 K. The aluminium mole fraction is $x = 0.26$ and 0.35, respectively. The same characteristics at 77 K are plotted in Fig. 7. The thickness of the AlGaAs layers varies from 3 to 6 μm. The data of our experiments are comparable to those of Collins *et al.* [19] and Ilegems [20]. Figure 8 and Table II show the influence of growth temperature on hole mobility and hole concentration. The beryllium cell temperature was kept at 580° C. It is known that

TABLE I Substrate temperature dependence of the doping concentration and electron mobility (silicon cell temperature is fixed at 910° C)

Sample	T_s (° C)	$n_{300\,K}$ (10^{17} cm^{-3})	$\mu_{300\,K}$ (cm^2 V^{-1} sec^{-1})	$n_{77\,K}$ (10^{16} cm^{-3})	$\mu_{77\,K}$ (cm^2 V^{-1} cm^{-1})
40916A	560	high resistance	–	high resistance	–
40916B	580	high resistance	–	high resistance	–
40923D	590	1.3	452	1.5	1700
40904A	620	2.0	700	3.0	4150
40923B	650	2.2	500	1.1	4900
40923F	680	4.5	930	3.4	1500

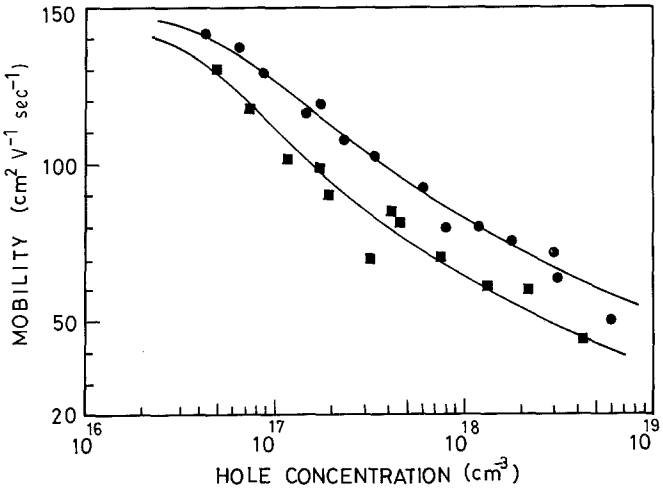

Figure 6 Hole mobility as a function of hole concentration at room temperature (300 K) in beryllium-doped $Al_xGa_{1-x}As$, where x = (●) 0.26, (■) 0.35.

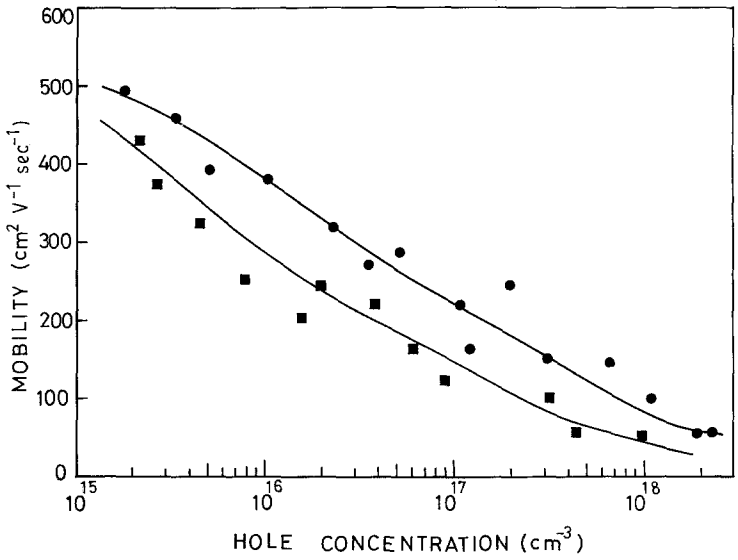

Figure 7 The relationship between the hole mobility and carrier concentration at 77 K, for beryllium-doped $Al_xGa_{1-x}As$, where x = (●) 0.26, (■) 0.35.

the relationship between the electrical properties and substrate temperature is not apparent, but when the substrate temperature is less than 580° C, it produces a semi-insulated high resistance, the same as that in silicon-doped AlGaAs layers. The undoped AlGaAs layer shows slight p-type characteristics due to the carbon acceptor. The carrier concentration of the unintentionally doped AlGaAs layers is smaller than $10^{15} cm^{-3}$.

3. Photoluminescent (PL) properties of $Al_xGa_{1-x}As$ layers

Low-temperature PL measurement has been used widely to analyse the optical properties of epitaxial layers [21]. Basically, the PL properties of AlGaAs layers are greatly affected by the quantities of residual gases (e.g. CO, H_2O) in the chamber, growth temperature and As/group-III flux ratio [18, 19, 22, 23]. Good vacuum conditions, high growth temperature and minimum arsenic vapour pressure are the conditions necessary for growing high-quality AlGaAs layers with excellent PL properties.

3.1. PL of undoped $Al_xGa_{1-x}As$ layers

Figure 9 illustrates the 14 K PL spectrum of undoped AlGaAs layers (x = 0.25 to 0.33) which were grown under different substrate temperatures. At the lower growth temperature, the bound exciton (Be) peak is

TABLE II Substrate temperature dependence of the doping concentration and hole mobility (beryllium-cell temperature is fixed at 585° C)

Sample	T_s (° C)	P_{300K} ($10^{17} cm^{-3}$)	μ_{300K} ($cm^2 V^{-1} sec^{-1}$)	p_{77K} ($10^{16} cm^{-3}$)	μ_{77K} ($cm^2 V^{-1} sec^{-1}$)
40924C	560	high resistance	–	high resistance	–
40926A	580	high resistance	–	high resistance	–
40924E	590	3.3	95	32	300
40925A	620	2.0	90	1.6	187
40924D	650	4.0	91	2.4	213
40925B	680	3.0	93	2.1	205

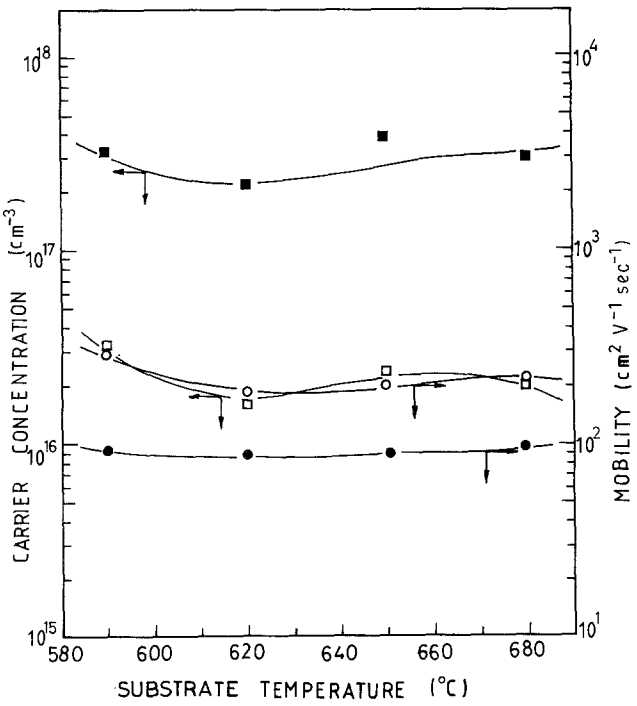

Figure 8 The influence of substrate temperature on electrical properties of beryllium doped $Al_{0.26}Ga_{0.74}As$ layers. Beryllium cell temperature = 585° C. (■,●) 300 K, (□, ○) 77 K.

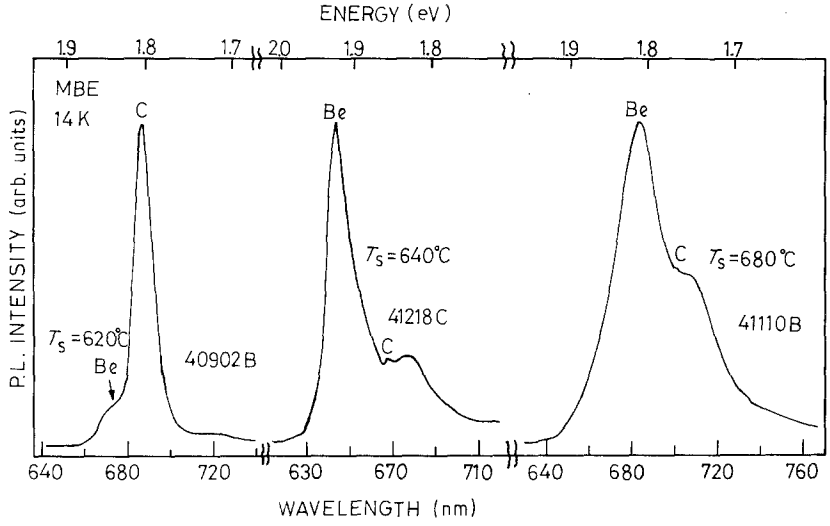

Figure 9 PL spectra of undoped $Al_xGa_{1-x}As$ layers under different growth temperatures.

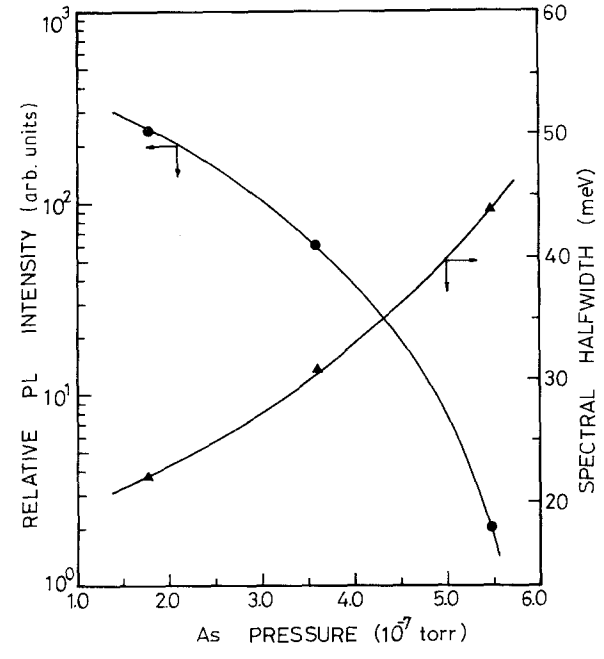

Figure 10 PL intensity in undoped $Al_{0.26}Ga_{0.74}As$ at 14 K as a function of arsenic partial pressure. Ar^+ = 488 nm, 60 mW.

not so apparent. The main peak is attributed to the D–A transition from the carbon acceptor. When the growth temperature is elevated, the Be peak becomes more apparent, i.e. the quality of the layers is improved. The small peak beside the C peak is carbon phonon replica (PH or C–LO), which is the main impurity of undoped AlGaAs layers and originated from the residual gases (e.g. CO, CO_2) in the growth chamber. In addition to carbon, oxygen also plays an important role in affecting the AlGaAs layer's quality, because oxygen can create a deep-level trap [24–26] and become an effective recombination centre, resulting mainly from CO and H_2O gases. So, good vacuum conditions play a very important role in the epitaxial layer's quality.

When the growth temperature is raised the desorption rate of Al_2O caused by oxygen is increased. Therefore, the influence of oxygen is reduced. Furthermore, the As_4 molecules can be desorbed into As_2 when the substrate temperature is elevated. From the analysis of Kunzel and Ploog [27], the layer's quality may be improved if As_4 is desorbed into As_2 during

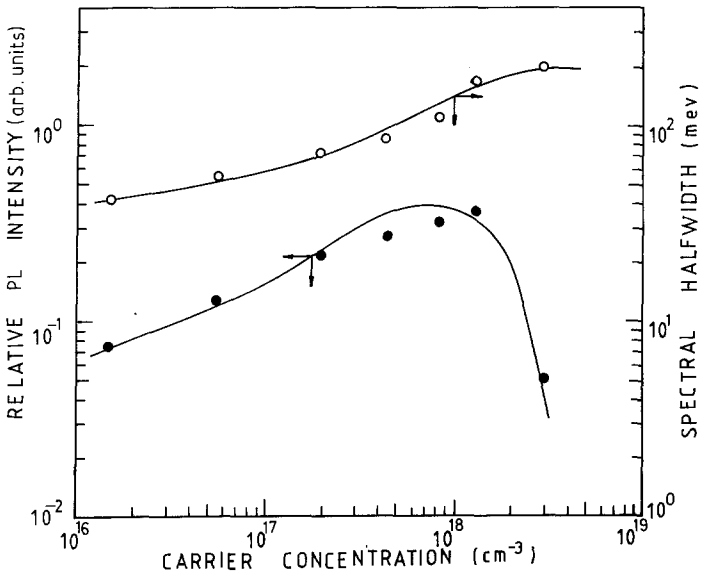

Figure 11 The influence of doping concentration on PL intensity and half width of silicon-doped $Al_xGa_{1-x}As$ layers at 14 K. Ar^+ = 488 nm, 60 mW.

MBE growth. So, a high substrate temperature is a necessary condition to obtain good PL properties.

The effect of arsenic partial pressure on PL is shown in Fig. 10. The substrate temperature was kept at 620° C. The arsenic partial pressure was increased from 1.8×10^{-7} to 5.5×10^{-7} torr. Significantly, the PL intensity is decreased drastically with increasing arsenic partial pressure. Furthermore, the halfwidth (FWHM) is increased by increasing the arsenic partial pressure. Therefore, the PL properties of undoped AlGaAs layers are degraded with increasing arsenic partial pressure, because many group-III vacancies are caused by too large an arsenic partial pressure and give rise to the formation of many nonradiative defects [23].

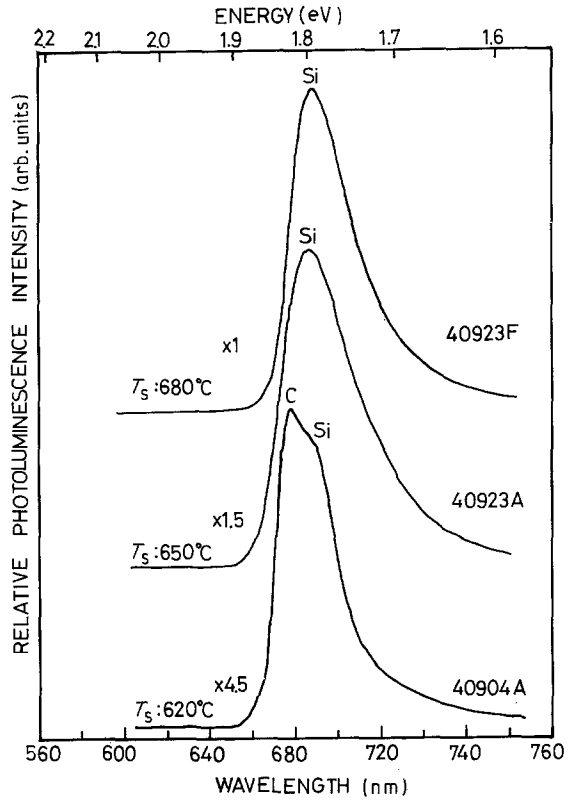

Figure 12 PL spectra of silicon-doped $Al_xGa_{1-x}As$ layers at 14 K under different growth temperatures. Ar^+ = 488 nm, 60 mW. $n_{300K} = 2 \times 10^{17} cm^{-3}$.

3.2. PL of silicon-doped $Al_xGa_{1-x}As$ layers

Figure 11 shows the relationship between the PL intensity, halfwidth and carrier concentration for silicon-doped $Al_xGa_{1-x}As$ (x = 0.25 to 0.33) layers. The doping level varied from 1.5×10^{16} to $3 \times 10^{18} cm^{-3}$ and the thickness of the epitaxial layers was about 1 to 3 μm. Initially, the PL efficiency increases with increasing doping concentration, but when the impurity density is higher than $10^{18} cm^{-3}$, the PL intensity decreases. This is because the recombination centres are increased with increasing doping concentration. So the PL efficiency is also increased. However, when the doping level is too high, the vacancies and nonradiative centres are increased due to impurity precipitation, which produces the degradation of PL intensity [28–30]. The halfwidth of the PL spectrum is increased with increasing doping concentration. Figure 12 illustrates the PL spectrum of silicon-doped $Al_xGa_{1-x}As$ layers grown under different substrate temperatures.

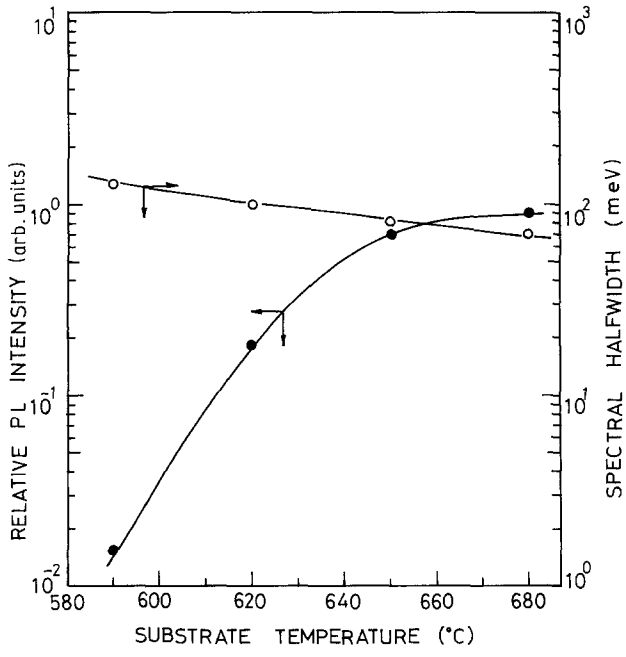

Figure 13 The influence of growth temperature on PL intensity and halfwidth of silicon-doped $Al_xGa_{1-x}As$ layers at 14 K, where $0.20 \leqslant x \leqslant 0.35$. Ar^+ = 488 nm, 60 mW. $n_{300K} = 2 \times 10^{17} cm^{-3}$.

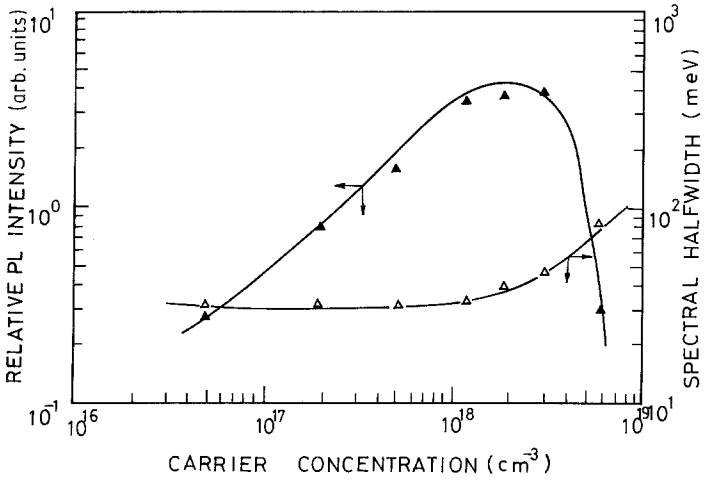

Figure 14 The influence of doping concentration on PL intensity and half width of beryllium-doped $Al_xGa_{1-x}As$ layers at 14 K. Ar^+ = 488 nm, 60 mW.

For comparison, the doping level was kept at $2 \times 10^{17}\,cm^{-3}$, and the thickness was about 3 μm. At lower growth temperatures (T_s = 620° C) the C peak is obvious, but it disappeared at higher growth temperatures. The influence of growth temperature on the PL intensity and half-width is depicted in Fig. 13. Significantly, the PL intensity and half-width increase and decrease, respectively, with increasing the substrate temperature. This proves that the elevation of substrate temperature can improve the PL properties of $Al_xGa_{1-x}As$ layers.

3.3. PL of beryllium-doped $Al_xGa_{1-x}As$ layers

Figure 14 shows the influence of carrier concentration on the relative PL intensity and spectral half width for beryllium-doped $Al_xGa_{1-x}As$ layers. Thickness of the epitaxial layers was about 3 μm and the substrate growth temperature was kept at 620° C. The AlAs mole fraction and carrier concentration varied from x = 0.2 to 0.35 and $p = 5 \times 10^{16}$ to $5.5 \times 10^{18}\,cm^{-2}$, respectively. Obviously, the PL intensity increases with increasing doping density, but when the impurity density is higher than $3 \times 10^{18}\,cm^{-3}$ it is reduced. The reason is the same as for silicon-doped layers, as mentioned above. The spectral half-width is increased with increasing doping level due to the increase in the number of recombination centres. Figure 15 shows the PL spectrum of beryllium-doped $Al_xGa_{1-x}As$ layers grown under different substrate temperatures. The doping level was kept to about $3 \times 10^{17}\,cm^{-3}$. Apparently, the spectrum becomes sharper at higher growth temperatures. When T_s = 590° C, an unidentified small peak is observed. Its origin is not yet clear: perhaps it is caused by some defects. The influence of substrate temperature on PL properties is depicted in Fig. 16. As predicted, the PL efficiency is increased with increasing substrate temperature. So, the high substrate temperature is a necessary condition to improve the PL properties. Basically, in our MBE system, the PL properties of beryllium-doped

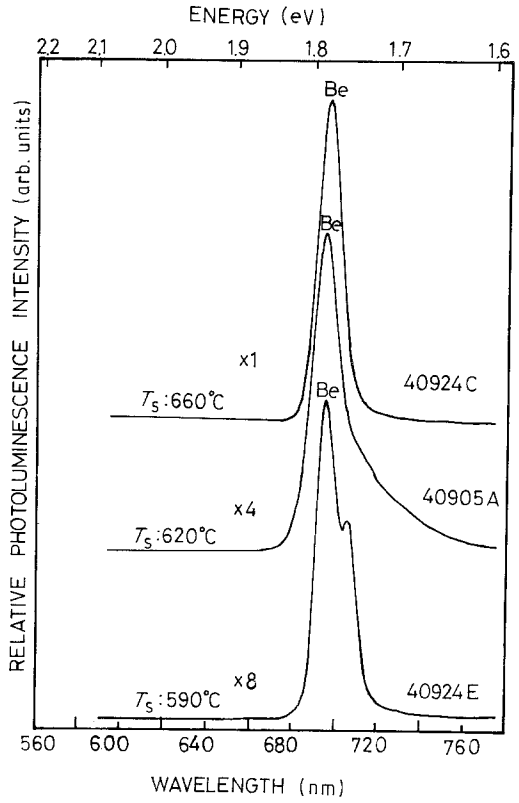

Figure 15 PL spectra of beryllium-doped $Al_xGa_{1-x}As$ layers at 14 K under different growth temperatures. Ar^+ = 488 nm, 60 mW. $p_{300\,K} = 3 \times 10^{17}\,cm^{-3}$.

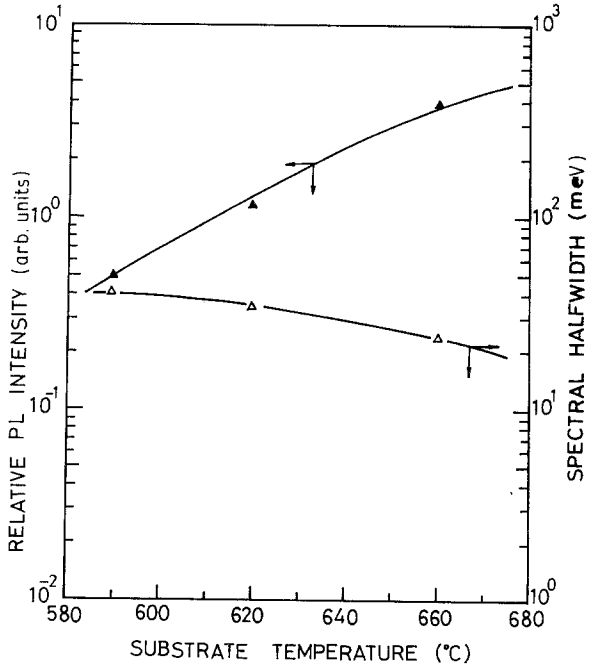

Figure 16 The influence of growth temperature on PL intensity and half width of beryllium-doped $Al_xGa_{1-x}As$ layers at 14 K, where $0.20 \leqslant x \leqslant 0.35$. $P_{300\,K} = 3 \times 10^{17}\,cm^{-3}$.

$Al_xGa_{1-x}As$ layers is superior to those of silicon-doped layers.

4. Conclusion

The electrical and PL properties of MBE-grown $Al_xGa_{1-x}As$ layers have been studied. Because elemental aluminium can react easily with oxygen, the improvement of vacuum conditions becomes an initial requirement for growing high-quality $Al_xGa_{1-x}As$ layers. Undoped AlGaAs layers exhibit p-type characteristics due to the carbon acceptor. Its concentration is lower than $10^{15}\,cm^{-3}$. In the electrical properties, both n- and p-type layers show a semi-insulated high resistance when the substrate growth temperature is lower than 580° C. The experimental results are comparable to other reports. Based on these techniques, some devices with $Al_xGa_{1-x}As$–GaAs heterostructure have been fabricated successfully in our laboratories [31–33]. In the PL properties, the substrate temperature and arsenic partial pressure play very important roles. Generally speaking, the PL properties of beryllium-doped AlGaAs layers are superior to silicon-doped AlGaAs layers in our experiments. In summary, the excellent vacuum environment, higher growth temperature (T_s > 580° C) and lower As/group-III flux ratio are the necessary conditions for growing high-quality $Al_xGa_{1-x}As$ layers.

References

1. A. Y. CHO, R. W. DIXON, H. C. CASEY Jr and R. L. HARTMANN, *Appl. Phys. Lett.* **28** (1976) 501.
2. W. T. TSANG, *ibid.* **34** (1979) 473.
3. P. M. SOLOMON and H. MORKOC, *IEEE Trans. Electron Device* **ED-31** (1984) 1015.
4. T. MIMURA, S. HIYAMIZU, T. FUJII and K. NANBU, *Jpn. J. Appl. Phys.* **24** (1980) L225.
5. W. T. TSANG, C. WEISBUCH, R. C. MILLER and R. DINGLE, *Appl. Phys. Lett.* **36** (1979) 673.
6. N. SUSA and H. OKAMOTO, *Jpn. J. Appl. Phys.* **23** (1984) 317.
7. H. MORKOC, T. J. DRUMMOND, W. KOOP and R. FISSCHER, *J. Electrochem. Soc.* **4** (1982) 824.
8. G. WICKS, W. I. WANG, C. E. C. WOOD, L. F. EASTMAN and L. RATHBUN, *J. Appl. Phys.* **52** (1981) 5792.
9. A. Y. CHO and J. R. ARTHUR, *Proc. Solid State Chem.* **10** (3) (1975) 157.
10. A. Y. CHO, *Thin Solid Films* **100** (1983) 291.
11. J. H. NEAVE, P. J. DOBSON, J. J. HARRIS, P. DAWSON and B. A. JOYCE, *Appl. Phys. A.* **32** (1983) 195.
12. A. CHANDRA and L. F. EASTMAN, *J. Electrochem. Soc.* **1** (1980) 211.
13. *Idem, J. Appl. Phys.* **51** (1980) 2669.
14. Y. G. CHAI, R. CHOW and C. E. C. WOOD, *Appl. Phys. Lett.* (1981) 800.
15. R. HECKINGBOTTOM and G. T. DAVIES, *J. Crystal Growth* **50** (1980) 644.
16. *Idem, J. Electrochem. Soc.* **127** (1980) 444.
17. A. MUNOZ-YANGE and S. BACEIREDO, *ibid.* **128** (1982) 2108.
18. J. M. BALLINGALL and D. M. COLLINS, *J. Appl. Phys.* **54** (1983) 341.
19. D. M. COLLINS, D. E. MARS and S. J. EGLASH, *J. Vac. Sci. Technol.* **B1** (1983) 170.
20. M. ILEGEMS, *J. Appl. Phys.* **48** (1982) 1278.
21. P. J. DEAN, *Proc. Crystal Growth Charact.* **5** (1982) 194.
22. V. SWAMINATHAN and W. T. TSANG, *Appl. Phys. Lett.* **38** (1981) 347.
23. W. T. TSANG and V. SWAMINATHAN, *ibid.* **39** (1981) 486.
24. K. HIKOSAKA, T. MIMURA and S. HIYAMIZU, *Inst. Phys. Ser.* **63** (1982) 233.
25. S. R. McAFEE, D. V. LANG and W. T. TSANG, *Appl. Phys. Lett.* **40** (1982) 520.
26. H. KINZEL, K. PLOOG, K. WUNSTEL and B. L. ZHOU, *J. Electron. Mater.* **13** (1984) 281.
27. H. KUNZEL and K. PLOOG, *Appl. Phys. Lett.* **37** (1980) 416.
28. G. B. STRINGFELLOW and R. LINNEBACH, *J. Appl. Phys.* **51** (1980) 2212.
29. V. SWAMINATHAN, N. E. SCHUMAKER, J. L. ZILKO, W. R. WAGNER and C. A. PARSONS, *ibid.* **52** (1981) 412.
30. V. SWAMINATHAN, M. D. STURGE and J. L. ZILKO, *ibid.* **52** (1981) 6306.
31. W. C. LIU, Y. H. WANG, C. Y. CHANG and S. A. LIAO, *IEE Proc. I. Solid State Electron.* **133** (1986) 47.
32. C. Y. CHANG, W. C. LIU and Y. H. WANG, Solid State Device and Materials Conference, Tokyo, Japan, August (1986) p. 20.
33. C. Y. WANG, W. C. LIU, M. S. JAME, Y. H. WANG, S. LURYI and S. M. SZE, *IEEE Electron Device Lett.* **EDL-7** (1986) 497.

Received 22 December 1988
and accepted 23 August 1989